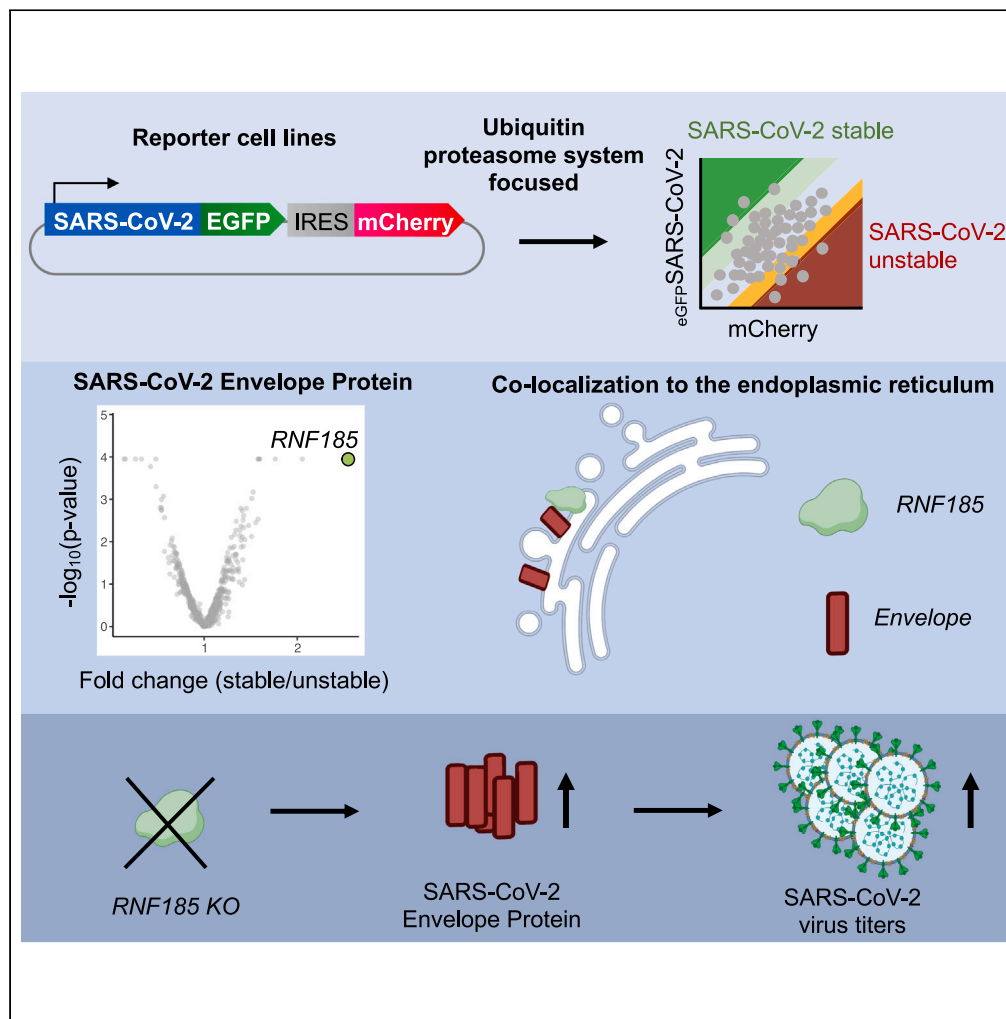


Article

The human E3 ligase RNF185 is a regulator of the SARS-CoV-2 envelope protein



Charles Zou,
Hojong Yoon, Paul
M.C. Park, ...,
Robert A. Davey,
Benjamin L. Ebert,
Mikołaj Słabicki

benjamin_ebert@dfci.harvard.edu (B.L.E.)
slabicki@broadinstitute.org (M.S.)

Highlights

RNF185, a human E3 ligase, regulates the stability of the SARS-CoV-2 envelope protein

RNF185 and the SARS-CoV-2 envelope protein co-localize at the endoplasmic reticulum

Depletion of RNF185 significantly increases SARS-CoV-2 viral titer in a cellular model



Article

The human E3 ligase RNF185 is a regulator of the SARS-CoV-2 envelope protein

Charles Zou,¹ Hojong Yoon,^{1,2} Paul M.C. Park,^{1,2} J.J. Patten,³ Jesse Pellman,^{1,2} Jeannie Carreiro,^{1,2} Jonathan M. Tsai,^{1,2} Yen-Der Li,^{1,2} Shourya S. Roy Burman,^{4,5} Katherine A. Donovan,^{4,5} Jessica Gasser,^{1,2} Adam S. Sperling,^{1,2,6} Radosław P. Nowak,^{4,5} Eric S. Fischer,^{4,5} Robert A. Davey,³ Benjamin L. Ebert,^{1,2,7,*} and Mikołaj Słabicki^{1,2,8,*}

SUMMARY

Severe acute respiratory syndrome coronavirus 2 (SARS-CoV-2) hijacks multiple human proteins during infection and viral replication. To examine whether any viral proteins employ human E3 ubiquitin ligases, we evaluated the stability of SARS-CoV-2 proteins with inhibition of the ubiquitin proteasome pathway. Using genetic screens to dissect the molecular machinery involved in the degradation of candidate viral proteins, we identified human E3 ligase RNF185 as a regulator of protein stability for the SARS-CoV-2 envelope protein. We found that RNF185 and the SARS-CoV-2 envelope co-localize to the endoplasmic reticulum (ER). Finally, we demonstrate that the depletion of RNF185 significantly increases SARS-CoV-2 viral titer in a cellular model. Modulation of this interaction could provide opportunities for novel antiviral therapies.

INTRODUCTION

Severe acute respiratory syndrome coronavirus 2 (SARS-CoV-2) is responsible for the current devastating global pandemic. While vaccines have achieved tremendous success, morbidity and mortality from SARS-CoV-2 continues to be a public health crisis due to evolution of new viral variants, infections in unvaccinated or immunocompromised individuals, and breakthrough infections in those who have been vaccinated.

Several SARS-CoV-2 antiviral therapies are in clinical use or development, including antibody cocktails that aim to block the receptor-binding domain of the SARS-CoV-2 spike protein¹, small molecules that inhibit the host RNA polymerase,^{2,3} small molecules that incorporate missense mutations into newly synthesized viral RNA,⁴ and small-molecule inhibitors of the viral main protease (MPro).⁵ Efforts to understand the viral cycle and map the function of each SARS-CoV-2 protein have identified potential antiviral targets.^{6,7} Comprehensive CRISPR-Cas9 screens have revealed several mammalian host genes critical for viral entry and replication including the ACE2 receptor,⁸ HMGB1, the SWI/SNF chromatin remodeling complex,⁹ and the lysosomal proteins TMEM106B¹⁰ and TMEM41B.¹¹

Some viral proteins modulate the ubiquitin-proteasome system (UPS) by redirecting E3 ubiquitin ligases to target and degrade host proteins, augmenting viral infection.¹² For example, the human papillomavirus E6 oncoprotein redirects the UBE3A ubiquitin ligase to induce degradation of the tumor suppressor p53.¹³ Among coronaviruses, SARS-CoV ORF-9b hijacks two ubiquitin ligases, PCBP2 and AIP4, to degrade MAVS, TRAF3, and TRAF6, thereby impairing the host interferon response.¹⁴ It was recently reported that SARS-CoV-2 ORF10 interacts with CUL2-ZYG11B,⁶ though it is not yet clear whether this interaction is required for infection.¹⁵ Though less well studied, it is also likely that host E3 ligases regulate viral protein stability, providing a mechanism for viral peptide quality control and clearance.

Targeted protein degradation has emerged as a powerful pharmacologic approach to alter the abundance of proteins in cells.^{16,17} One potential antiviral strategy is to modulate the interaction of a viral protein with a host ubiquitin ligase using a small molecule to promote its removal by the UPS. We used CRISPR screens to identify SARS-CoV-2 proteins targeted for degradation by human E3 ubiquitin ligases. Such E3 ligase-viral

¹Department of Medical Oncology, Dana-Farber Cancer Institute, Boston, MA 02215, USA

²Broad Institute of MIT and Harvard, Cambridge, MA, USA

³Department of Microbiology, Boston University School of Medicine and NEIDL, Boston University, Boston, MA 02118, USA

⁴Department of Cancer Biology, Dana-Farber Cancer Institute, Boston, MA 02215, USA

⁵Department of Biological Chemistry and Molecular Pharmacology, Harvard Medical School, Boston, MA 02115, USA

⁶Division of Hematology, Department of Medicine, Brigham and Women's Hospital, Harvard Medical School, Boston, MA, USA

⁷Howard Hughes Medical Institute, Boston, MA, USA

⁸Lead contact

*Correspondence: benjamin_ebert@dfci.harvard.edu (B.L.E.), slabicki@broadinstitute.org (M.S.)

<https://doi.org/10.1016/j.isci.2023.106601>



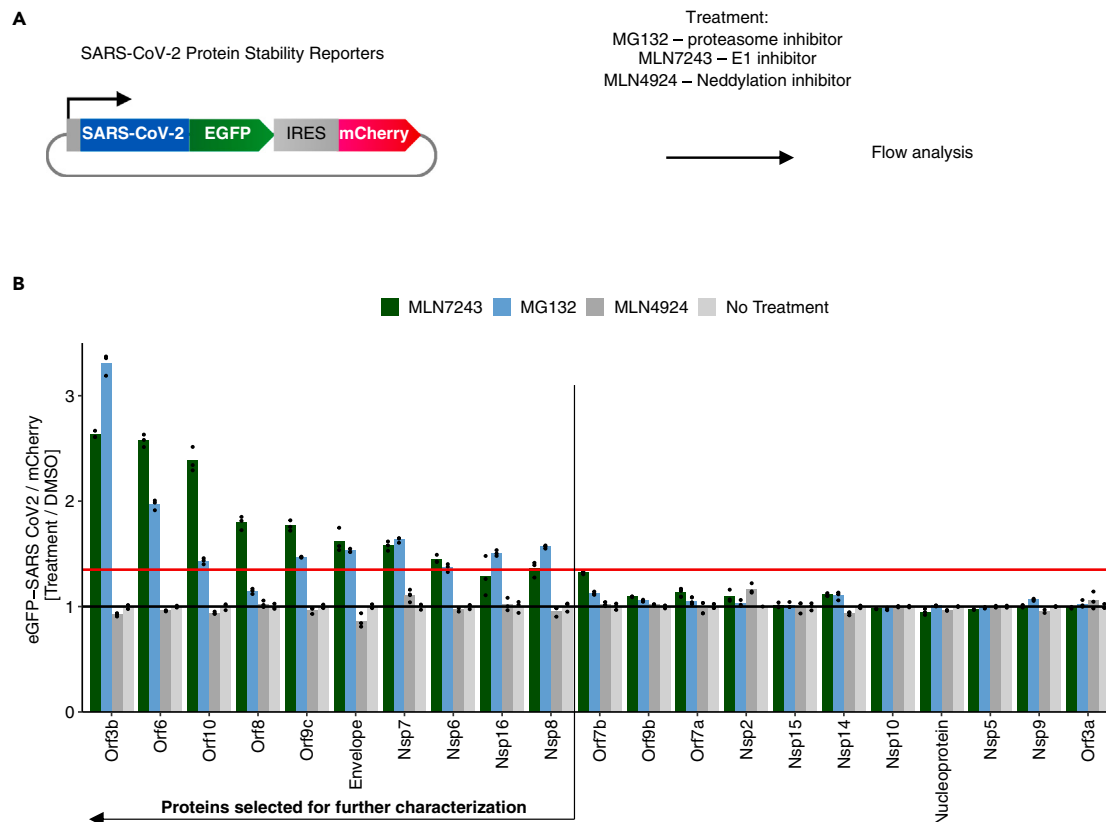


Figure 1. The stability of SARS-CoV-2 proteins in HEK293T cells

(A) Schematic overview of protein stability assay for SARS-CoV-2 proteins.

(B) Flow cytometry analysis of SARS-CoV-2 protein stability reporters after 6 h of treatment with 10 μ M of MG132, 1 μ M MLN7243, 1 μ M MLN4924, or DMSO (bars represent mean, n = 3). Black line represents mean eGFP/mCherry expression of non-treated cells; red line represents a 30% increase of expression.

protein interacting pairs can serve as starting points for the identification of molecular glues that strengthen such interactions and boost antiviral activity.

RESULTS

Identification of SARS-CoV-2 proteins degraded by the human ubiquitin-proteasome system

We first sought to identify SARS-CoV-2 proteins that are degraded by human E3 ubiquitin ligases. To monitor the stability of SARS-CoV-2 proteins, we generated a set of fluorescent reporter constructs. Each construct contains the sequence of a single, full-length SARS-CoV-2 protein fused in-frame with GFP, eGFP, followed by an internal ribosome entry site and red fluorescent protein, mCherry, for signal normalization (Figure 1A).¹⁸ Out of 28 SARS-CoV-2 proteins, we successfully generated 21 reporter cell lines in human HEK293T cells (Table S1).

To test whether stability of the viral proteins is influenced by the UPS, we treated reporter-expressing cells with a ubiquitin-activating enzyme inhibitor (MLN7243), a 26S proteasome inhibitor (MG132), or a neddylation inhibitor (MLN4924), and monitored eGFP/mCherry expression levels of treated cells using flow cytometry normalized to untreated controls (Figure 1B). Inhibitor treatment affected the levels of eGFP-SARS-CoV-2 proteins without affecting the mCherry controls (Figure S1). If the levels of eGFP/mCherry expression increased over 30% upon inhibitor treatment (p value <0.01), we considered the SARS-CoV-2 protein reporter to be destabilized by the human UPS. As expected, all reporters that were stabilized by MLN7243 E1 inhibitor treatment were also stabilized by inhibition of proteasome with MG132. Treatment with MLN4924, however, did not change the stability of any SARS-CoV-2 eGFP fusions, indicating that no SARS-CoV-2 proteins are degraded by cullin ring E3 ligases in the cell line tested.¹⁹ By our criteria, ten out of the twenty-one SARS-CoV-2 fusion proteins tested here are degraded by the human UPS (Figure 1B).

Genetic screens for human E3 ligases that destabilize SARS-CoV-2 proteins

We next sought to identify the specific E3 ubiquitin ligase components responsible for destabilization of the ten identified SARS-CoV-2 proteins. We transduced the reporter-expressing HEK293T cell line with a single-guide RNA (sgRNA) library targeting ~700 E3 ligases, E2 conjugating enzymes, and deubiquitinating enzymes (DUBs).^{20,21} The fluorescent reporter cell lines were sorted into four populations based on eGFP/mCherry ratio ((Gate A) bottom 5%, (Gate B) bottom 5%–10%, (Gate C) top 5%–10%, (Gate D) top 5%) (Figure 2A). Cells sorted into Gates A and B had reduced eGFP/mCherry expression, indicating relatively enhanced degradation of the SARS-CoV-2 eGFP fusion protein, whereas cells sorted into Gates C and D had relatively increased stability of SARS-CoV-2 eGFP fusion protein. After sorting, cell pellets were lysed and sgRNAs were amplified and quantified by next-generation sequencing. We compared sgRNAs read counts from the SARS-CoV-2 most stable population (Gate D) to the most unstable population (Gate A).

For eight out of the ten SARS-CoV-2 protein reporters screened, the genetic screen revealed significant enrichment for at least one E3 ligase (Figures 2B, 2C and S2). Two of the most significantly enriched ligases in the stable population compared to the unstable population were RNF185, in the SARS-CoV-2 envelope-eGFP screen (Figure 2B), and SYVN1, in the SARS-CoV-2 Orf8-eGFP screen (Figure S3A). The E3 ubiquitin-protein ligase UBE3C, which scored in six screens, has been shown to influence the rate of degradation for domains fused to eGFP,²² and was therefore excluded as a potential assay artifact.

Validation of E3 ligases that induce degradation of SARS-CoV-2 proteins

We next validated the two identified pathogen-host pairs, envelope – RNF185 and Orf8 – SYVN1, in additional cellular contexts. We tested the effect of UPS inhibitors on the stability of envelope-eGFP and Orf8-eGFP fusions in A549 (lung epithelial) cells and K562 (acute myeloid leukemia) cells. We treated the reporter cell lines with a set of ubiquitin-proteasome inhibitors and monitored the levels of SARS-CoV-2 eGFP fusion. For the SARS-CoV-2 envelope protein, we observed an increase of protein stability in A549 and K562 cells upon the treatment with MLN7243 and MG132 (p.value <0.01), but not MLN4924, consistent with the results for HEK293T cells (Figures S3B and S3C). The SARS-CoV-2 Orf8 protein was stabilized upon MLN7243 and MG132 treatment in HEK293T and K562 cells, but not in the A549 cell line (Figure S3D), suggesting that one or more factors were needed to regulate the envelope protein, and that ORF8 is differentially expressed in these cell lines.

We next sought to validate the E3 ligases that scored in our genetic screens, RNF185 and SYVN1, by targeting them with multiple independent sgRNAs in three cell lines. We knocked out *RNF185* and *SYVN1* with four sgRNAs each and compared the levels of SARS-CoV-2 envelope protein or Orf8 in the eGFP/mCherry expression system to a non-targeting control guide by flow cytometry. CRISPR-Cas9 knockout of RNF185 efficiently depleted RNF185 protein levels (Figure 2D), which resulted in increased expression of SARS-CoV-2 envelope-eGFP by 2- to 3-fold in all cell lines tested (p.value <0.01) (Figure 2E), validating the involvement of RNF185 in the stability of the envelope protein. The knockout of SYVN1 in HEK293T and K562 cells significantly increased levels of SARS-CoV-2 Orf8-GFP (Figure S3D), but not in A549 cells.

RNF185 colocalizes with the SARS-CoV-2 envelope protein

Since RNF185 knockout consistently rescued envelope protein degradation across multiple individual sgRNAs and three cell lines, we decided to focus on this E3 ligase. RNF185 has previously been shown to form an endoplasmic reticulum (ER)-associated protein degradation (ERAD) complex involved in quality control of proteins on the ER membrane.^{23,24} To investigate the cellular localization of the RNF185 and envelope proteins, HEK293T cells stably expressing the SARS-CoV-2 envelope-eGFP fusion protein cells were transfected with a RNF185-iRFP720 fusion construct and stained with an ER dye. RNF185 and the SARS-CoV-2 envelope protein partially co-localized with the ER marker (Figure 3A).

Prior studies have demonstrated that TMEM259 is necessary for ubiquitin ligase RNF185 function in the context of the ERAD complex for the quality control of membrane proteins.²³ To examine whether this complex is needed for targeting the viral envelope protein, we used CRISPR-Cas9 to knock out TMEM259 and monitored SARS-CoV-2 envelope protein levels by flow cytometry. Depletion of TMEM259 by sgRNAs increased the stability of SARS-CoV-2 envelope protein (Figure 3B), confirming that an ERAD complex member is involved in modulating SARS-CoV-2 envelope levels.

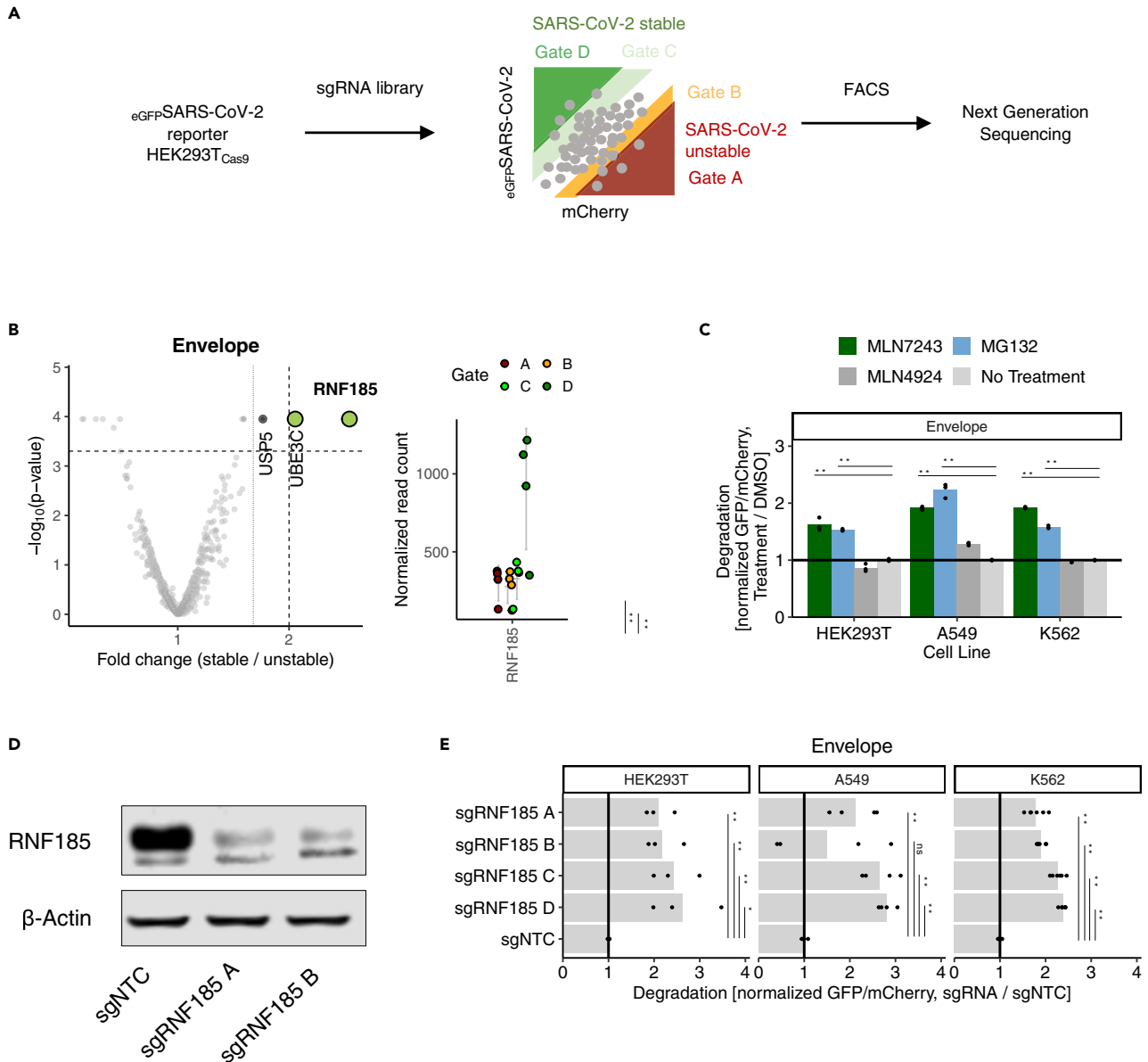


Figure 2. Functional genomic screens identified RNF185 ligases for SARS-CoV-2 envelope stability

(A) Schematic of CRISPR sorting screen of the SARS-CoV-2 protein stability. Reporter cell lines were transduced with Bison CRISPR sgRNA library (713 E1, E2, and E3 ubiquitin ligases, deubiquitinases, and control genes containing 2,852 sgRNAs), cultured for 8 days, then sorted into 4 gates based on GFP/mCherry ratio. (Gate A: bottom 0%–5%; Gate B: bottom 5%–10%; Gate C: top 90%–95%; Gate D: top 95%–100%).

(B) CRISPR-Cas9 sorting screen for cells with altered stability of SARS-CoV-2 envelope. Guides were collapsed to gene levels (n = 2, four guides per gene, two-sided empirical ran-sum test-statistic, horizontal dashed line indicates p value = 0.0005, vertical dashed line indicates fold change of 2, vertical dot line indicates fold change of 1.6). Normalized read count for sgRNAs targeting RNF185 is shown.

(C) Flow cytometry analysis of degradation of SARS-CoV-2 envelope in a panel of three cell lines after 6 h of treatment with 10 μM of MG132, 1 μM MLN7243, 1 μM MLN4924, or DMSO (** p value <0.01, ns – not significant).

(D) Immunoblots of RNF185 levels after infection with sgRNF185 or sgNTC.

(E) Flow cytometry analysis of SARS-CoV-2 envelope reporter stability following single-guide knockout of RNF185 across three different cell lines (* p value <0.05, ** p value <0.01).

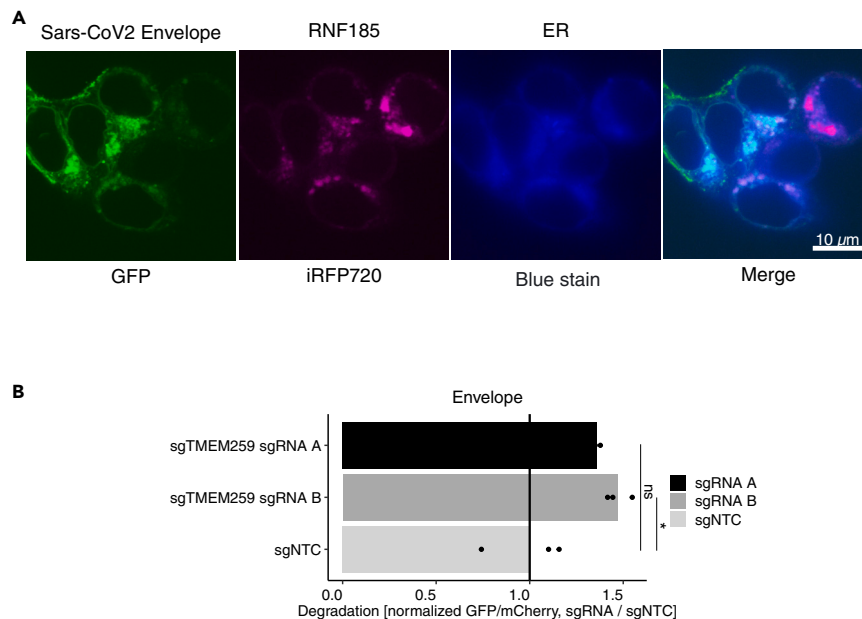


Figure 3. Degradation of SARS-CoV-2 envelope protein is mediated by RNF185/TMEM259 complex

(A) Fluorescent microscopy of HEK293T cells transiently transfected with iRFP720 tagged RNF185 and GFP tagged envelope proteins.

(B) Flow cytometry analysis of CRISPR-Cas9 knocked out TMEM259 compared to a non-targeting control.

RNF185 is involved in the degradation of SARS-CoV-2 clinical variants as well as SARS-CoV envelope proteins

Since initial isolation of SARS-CoV-2, the envelope protein has been one of the most rapidly evolving proteins for subsequent variants of the virus. The most common mutations in the SARS-CoV-2 envelope protein are in the C-terminus of the protein (amino acids (aa) 55–73) and the transmembrane domain (aa 9). To test whether RNF185 is still able to modulate envelope protein levels in these variants, we expressed them as eGFP fusions in HEK293T cells. Depletion of RNF185 increases the levels of SARS-CoV-2 envelope for all variants tested (Figure 4A).

SARS-CoV is closely related to SARS-CoV-2 and their envelope proteins share a high degree of protein sequence homology (91% sequence identity), while the MERS envelope protein is more distinct (35% sequence identity) (Figure 4B). Having observed RNF185-mediated degradation of the SARS-CoV-2 envelope protein, we sought to determine whether degradation of the SARS-CoV and MERS envelope proteins is mediated by the same E3 ligase. The SARS-CoV and MERS envelope proteins were fused to eGFP in our reporter vector and expressed in HEK293T cells. We observed that sgRNA targeting RNF185 stabilized protein levels for both the SARS-CoV-2 and the SARS-CoV envelope proteins, albeit to a greater degree for SARS-CoV-2, indicating that RNF185 is involved in the degradation of the envelope protein of both SARS viruses. In contrast, the MERS envelope protein stability was not affected by RNF185 depletion (Figure 4C) consistent with observed differences between the sequences of the envelope protein in MERS compared to that of SARS-CoV and SARS-CoV-2.

RNF185 knockout increases SARS-CoV-2 viral titer

To examine whether RNF185 is relevant to SARS-CoV-2 virus production, we examined viral titer in host cells with RNF185 inactivation. We knocked out RNF185 in A549-ACE2 cells using CRISPR/Cas9 and infected the cells with three SARS-CoV-2 strains: WA, Beta, or Delta.²⁵ Three days following infection, viral titers were measured by a PCR release assay. Knockout of RNF185 resulted in a ~60% increase in viral titers for all three SARS-CoV-2 strains which was statistically significant for the Beta and Delta variants (Figure 5).

DISCUSSION

In this study, we systematically examined whether SARS-CoV-2 proteins are destabilized by human E3 ubiquitin ligases, and we report that RNF185 induces degradation of the SARS-CoV-2 envelope protein. We

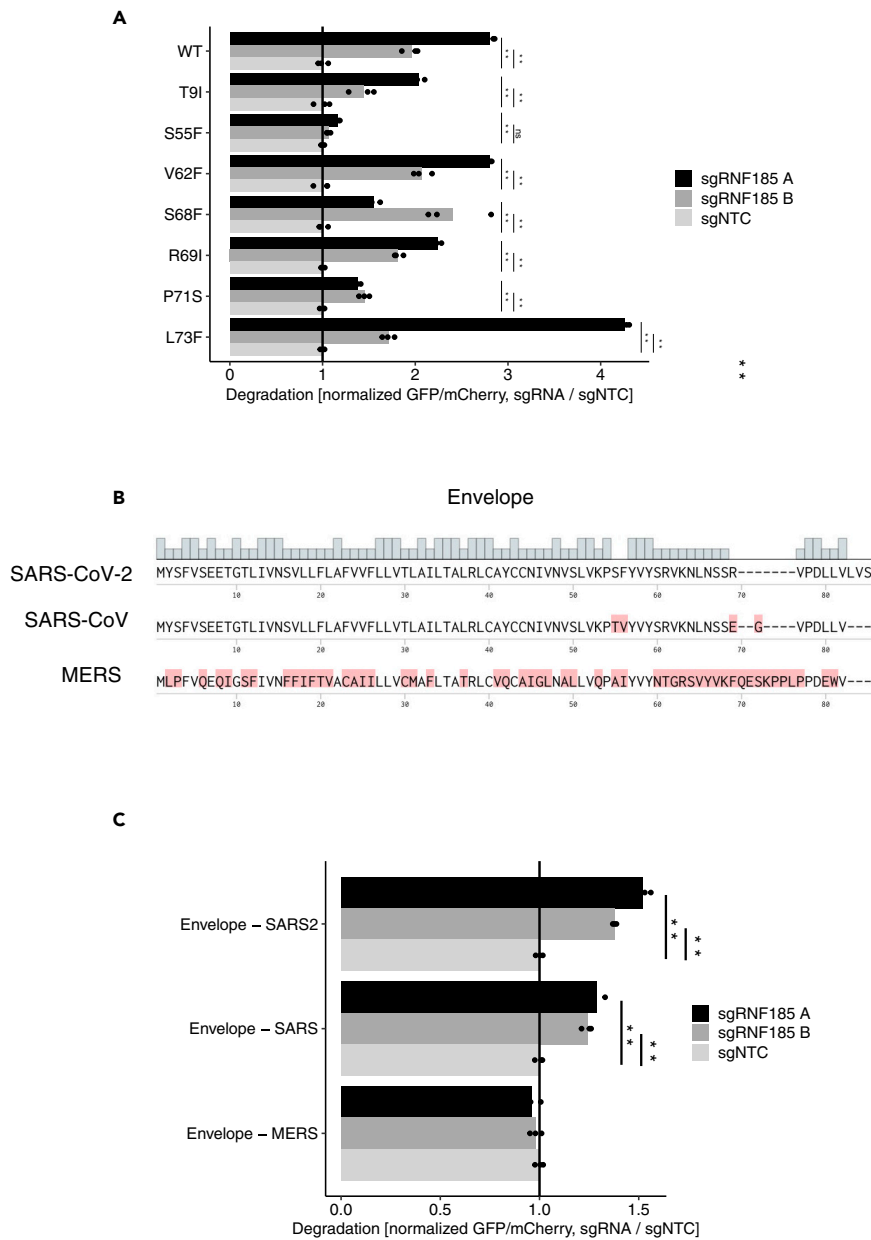


Figure 4. RNF185-mediated degradation of the envelope protein is seen in SARS-CoV-2 wild-type, clinical variants as well as SARS-CoV but not MERS

(A) Flow cytometry analysis of degradation of clinical variants of SARS-CoV-2 envelope protein following infection of CRISPR guides targeting RNF185.

(B) Sequence alignment of envelope protein for SARS-CoV-2, SARS-CoV, and MERS.

(C) Flow cytometry analysis of degradation of SARS-CoV-2, SARS-CoV, and MERS envelope protein following infection of CRISPR guides targeting RNF185.

demonstrated that the SARS-CoV-2 envelope colocalizes with RNF185. Furthermore, depletion of TMEM259, a member of the ERAD complex required for RNF185 function, phenocopies the effect of RNF185 knockout. Our results demonstrate that RNF185 modulates envelope protein levels for several SARS-CoV-2 clinical variants and for SARS-CoV, but not for MERS. Finally, in viral titer assays, depletion of RNF185 increased viral titer, demonstrating that the role of RNF185 in regulating envelope protein levels has biological consequences for virus production.

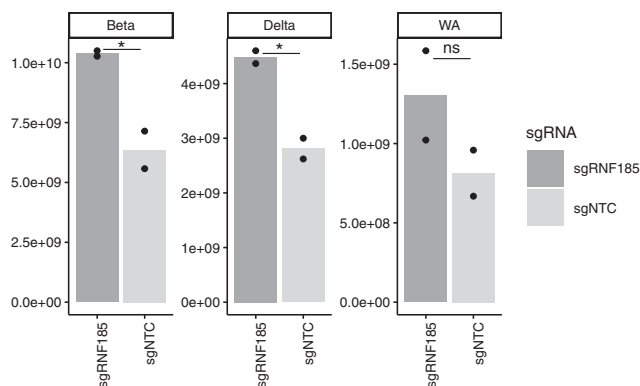


Figure 5. SARS-CoV-2 virus titers in A549-ACE2 cell line upon RNF185 depletion

Virus titers were measured by detection of genomes in culture supernatants by PCR-based assay (* p value <0.05, ns – not significant). Titters are expressed as genome equivalents per mL of culture supernatant.

RNF185 is a non-cullin E3 ubiquitin ligase that is part of the ERAD family of E3 ligases and is important for quality control of ER-synthesized proteins, targeting misfolded or unfolded proteins for degradation to reduce cellular stress.²³ RNF185 was previously implicated in cGAS-mediated innate immune response upon HSV-1 infection,²² suggesting that RNF185 may be more broadly involved in viral pathogenic processes.

The SARS-CoV-2 envelope protein is synthesized in the ER and subsequently trafficked to the Golgi and ER-Golgi intermediate compartment where it is involved in multiple steps of the viral life cycle: viral assembly, budding, viral release, and inflammasome activation.²⁶ Our results indicate that RNF185 is involved in degradation of the envelope protein. The SARS-CoV-2 envelope protein has been suggested to be a good target for an antiviral therapeutic that induces protein degradation as it would inhibit viral entry, replication, and assembly.²⁷

In multiple cases, a small molecule can augment ubiquitination by a protein's cognate E3 ligase. For example, small-molecule-induced polymerization of the transcriptional repressor BCL6 leads to its enhanced ubiquitination and degradation by the E3 ligase SIAH1,¹⁹ and small-molecule enhancement of the protein-protein interaction between the transcription factor β -catenin and its endogenous E3 ligase SCF ^{β -TrCP}²⁸ leads to degradation of β -catenin. A small molecule that increases the affinity of the SARS-CoV-2 envelope protein to RNF185 could be an effective antiviral treatment strategy to reduce the effective concentration of viral structural components, lowering the barrier to ubiquitination and clearance. In addition, a small-molecule binder to the envelope protein could increase the retention time of the SARS-CoV-2 envelope protein in the ER, leading to enhanced degradation by the RNF185 E3 ubiquitin ligase. The finding that RNF185 degrades SARS-CoV-2 envelope protein provides a rationale for seeking small molecules that strengthen this interaction, thereby enhancing degradation of the SARS-CoV-2 envelope protein, resulting in antiviral activity.

Limitations of the study

A potential limitation of this study is that we only evaluated the stability of SARS-CoV-2 proteins in human HEK293T cells, which may not fully represent the diverse range of host cells and tissues infected by the virus *in vivo*. While this study identified a potential target for antiviral therapeutics, additional research is required to explore the biochemical and structural basis for the impact of RNF185 on SARS-CoV-2 envelope protein stability and the therapeutic potential of modulating the interaction between RNF185 and the envelope protein.

STAR★METHODS

Detailed methods are provided in the online version of this paper and include the following:

- KEY RESOURCES TABLE
- RESOURCE AVAILABILITY
- Lead contact

- Material availability
- Data and code availability
- **EXPERIMENTAL MODEL AND SUBJECT DETAILS**
 - Cell lines
 - Generation of stability constructs
 - Lentivirus production
 - Lentiviral transduction
 - SARS-CoV-2 stability assay
 - BISON SARS-CoV-2 reporter screen in HEK293T cells
 - Data analysis of CRISPR-Cas9 knockout screens
 - Generation of CRISPR-Cas9 knock-out cells
 - Immunoblots
 - Transient transfection
 - Fluorescence microscopy
 - Virus cultivation
 - Effect of RNF185 KO on SARS-CoV-2 replication

SUPPLEMENTAL INFORMATION

Supplemental information can be found online at <https://doi.org/10.1016/j.isci.2023.106601>.

ACKNOWLEDGMENTS

M.S. is supported by Scientific Projects to Accelerate Research and Collaboration (Broad Institute). H.Y. is supported by NIH grant NCI K00CA253754. J.J.P. and R.A.D. were supported by a grant from MassCPR. A.S.S. was supported by NCI grant K08-CA252174 and DOD grant CA21827. We are grateful to Nathanael S. Gray and all members of the Ebert laboratory for discussion, particularly, Peter G. Miller, Roger Belizaire, Marek Nagiec, and Christopher Hergott.

AUTHOR CONTRIBUTIONS

M.S., C.Z., B.L.E. conceptualized and initiated the study; M.S. designed, and C.Z. performed experiments with the help of H.Y., P.M.C.P., J.J.P., J.P., J.C., J.M.T., Y.D.L., S.S.R.B., K.A.D., J.G., A.S.S., R.P.N. M.S., B.L.E., R.P.N., E.S.F., R.A.D. supervised the project. M.S., C.Z., B.L.E. wrote the manuscript with input from all authors.

DECLARATION OF INTERESTS

M.S. has received research funding from Calico Life Sciences LLC. B.L.E. has received research funding from Celgene, Deerfield, Novartis, and Calico Life Sciences LLC and consulting fees from GRAIL. He is a member of the scientific advisory board and shareholder for Neomorph Inc., TenSixteen Bio, Skyhawk Therapeutics, and Exo Therapeutics. E.S.F. is a founder, member of the scientific advisory board (SAB), and equity holder of Civetta Therapeutics, Proximity Therapeutics, and Neomorph Inc (also board of directors), a SAB member and equity holder in Avilar Therapeutics and Photys Therapeutics, equity holder in Lighthouse Therapeutics, and a consultant to Sanofi, Novartis, Deerfield, Odyssey Therapeutics, and EcoR1 capital. The Fischer laboratory receives or has received research funding from Novartis, Deerfield, Ajax, Interline, and Astellas. K.A.D. is a consultant to Kronos Bio and Neomorph Inc. A.S.S. reports consulting fees from Adaptive Technologies and Roche.

INCLUSION AND DIVERSITY

We support inclusive, diverse, and equitable conduct of research.

Received: March 31, 2022

Revised: January 31, 2023

Accepted: March 29, 2023

Published: April 8, 2023

REFERENCES

- Weinreich, D.M., Sivapalasingam, S., Norton, T., Ali, S., Gao, H., Bhore, R., Musser, B.J., Soo, Y., Rofail, D., Im, J., et al.; Trial Investigators (2021). REGN-COV2, a neutralizing antibody cocktail, in outpatients with Covid-19. *N. Engl. J. Med.* 384, 238–251.
- Caly, L., Druce, J.D., Catton, M.G., Jans, D.A., and Wagstaff, K.M. (2020). The FDA-approved drug ivermectin inhibits the replication of SARS-CoV-2 in vitro. *Antiviral Res.* 178, 104787.
- Wang, M., Cao, R., Zhang, L., Yang, X., Liu, J., Xu, M., Shi, Z., Hu, Z., Zhong, W., and Xiao, G. (2020). Remdesivir and chloroquine effectively inhibit the recently emerged novel coronavirus (2019-nCoV) in vitro. *Cell Res.* 30, 269–271.
- Sheahan, T.P., Sims, A.C., Zhou, S., Graham, R.L., Pruijssers, A.J., Agostini, M.L., Leist, S.R., Schäfer, A., Dinnon, K.H., 3rd, Stevens, L.J., et al. (2020). An orally bioavailable broad-spectrum antiviral inhibits SARS-CoV-2 in human airway epithelial cell cultures and multiple coronaviruses in mice. *Sci. Transl. Med.* 12, eabb5883.
- Owen, D.R., Allerton, C.M.N., Anderson, A.S., Aschenbrenner, L., Avery, M., Berritt, S., Boras, B., Cardin, R.D., Carlo, A., Coffman, K.J., et al. (2021). An oral SARS-CoV-2 M(pro) inhibitor clinical candidate for the treatment of COVID-19. *Science* 374, 1586–1593.
- Gordon, D.E., Jang, G.M., Bouhaddou, M., Xu, J., Obernier, K., O’Meara, M.J., Guo, J.Z., Swaney, D.L., Tummino, T.A., Huttenhain, R., et al. (2020). A SARS-CoV-2-human protein-protein interaction map reveals drug targets and potential drug-repurposing. *Nature* 583, 459–468.
- Gordon, D.E., Jang, G.M., Bouhaddou, M., Xu, J., Obernier, K., White, K.M., O’Meara, M.J., Rezelj, V.V., Guo, J.Z., Swaney, D.L., et al. (2020). A SARS-CoV-2 protein interaction map reveals targets for drug repurposing. *Nature* 583, 459–468.
- Zhu, Y., Feng, F., Hu, G., Wang, Y., Yu, Y., Zhu, Y., Xu, W., Cai, X., Sun, Z., Han, W., et al. (2021). A genome-wide CRISPR screen identifies host factors that regulate SARS-CoV-2 entry. *Nat. Commun.* 12, 961.
- Wei, J., Alfajaro, M.M., DeWeirdt, P.C., Hanna, R.E., Lu-Culligan, W.J., Cai, W.L., Strine, M.S., Zhang, S.M., Graziano, V.R., Schmitz, C.O., et al. (2021). Genome-wide CRISPR screens reveal host factors critical for SARS-CoV-2 infection. *Cell* 184, 76–91.e13.
- Baggen, J., Persoons, L., Vanstreels, E., Jansen, S., Van Looveren, D., Boeckx, B., Geudens, V., De Man, J., Jochmans, D., Wauters, J., et al. (2021). Genome-wide CRISPR screening identifies TMEM106B as a proviral host factor for SARS-CoV-2. *Nat. Genet.* 53, 435–444.
- Schneider, W.M., Luna, J.M., Hoffmann, H.H., Sánchez-Rivera, F.J., Leal, A.A., Ashbrook, A.W., Le Pen, J., Ricardo-Lax, I., Michailidis, E., Peace, A., et al. (2021). Genome-scale identification of SARS-CoV-2 and pan-coronavirus host factor networks. *Cell* 184, 120–132.e14.
- Mahon, C., Krogan, N.J., Craik, C.S., and Pick, E. (2014). Cullin E3 ligases and their rewiring by viral factors. *Biomolecules* 4, 897–930.
- Scheffner, M., Huijbregtse, J.M., Vierstra, R.D., and Howley, P.M. (1993). The HPV-16 E6 and E6-AP complex functions as a ubiquitin-protein ligase in the ubiquitination of p53. *Cell* 75, 495–505.
- Shi, C.S., Qi, H.Y., Boularan, C., Huang, N.N., Abu-Asab, M., Shelhamer, J.H., and Kehrl, J.H. (2014). SARS-coronavirus open reading frame-9b suppresses innate immunity by targeting mitochondria and the MAVS/TRAF3/TRAF6 signalosome. *J. Immunol.* 193, 3080–3089.
- Mena, E.L., Donahue, C.J., Vaites, L.P., Li, J., Rona, G., O’Leary, C., Lignitto, L., Miwatani-Minter, B., Paulo, J.A., Dhabaria, A., et al. (2021). ORF10-Cullin-2-ZYG11B complex is not required for SARS-CoV-2 infection. *Proc. Natl. Acad. Sci. USA* 118, e2023157118.
- Mullard, A. (2021). Targeted protein degraders crowd into the clinic. *Nat. Rev. Drug Discov.* 20, 247–250.
- Jan, M., Sperling, A.S., and Ebert, B.L. (2021). Cancer therapies based on targeted protein degradation - lessons learned with lenalidomide. *Nat. Rev. Clin. Oncol.* 18, 401–417.
- Yen, H.C.S., Xu, Q., Chou, D.M., Zhao, Z., and Elledge, S.J. (2008). Global protein stability profiling in mammalian cells. *Science* 322, 918–923.
- Soucy, T.A., Smith, P.G., Milhollen, M.A., Berger, A.J., Gavin, J.M., Adhikari, S., Brownell, J.E., Burke, K.E., Cardin, D.P., Critchley, S., et al. (2009). An inhibitor of NEDD8-activating enzyme as a new approach to treat cancer. *Nature* 458, 732–736.
- Slabicki, M., Kozicka, Z., Petzold, G., Li, Y.D., Manojkumar, M., Bunker, R.D., Donovan, K.A., Sievers, Q.L., Koepfel, J., Suchyta, D., et al. (2020). The CDK inhibitor CR8 acts as a molecular glue degrader that depletes cyclin K. *Nature* 585, 293–297.
- Slabicki, M., Yoon, H., Koepfel, J., Nitsch, L., Roy Burman, S.S., Di Genua, C., Donovan, K.A., Sperling, A.S., Hunkeler, M., Tsai, J.M., et al. (2020). Small-molecule-induced polymerization triggers degradation of BCL6. *Nature* 588, 164–168.
- Chu, B.W., Kovary, K.M., Guillaume, J., Chen, L.C., Teruel, M.N., and Wandless, T.J. (2013). The E3 ubiquitin ligase UBE3C enhances proteasome processivity by ubiquitinating partially proteolyzed substrates. *J. Biol. Chem.* 288, 34575–34587.
- El Khouri, E., Le Pavec, G., Toledano, M.B., and Delaunay-Moisan, A. (2013). RNF185 is a novel E3 ligase of endoplasmic reticulum-associated degradation (ERAD) that targets cystic fibrosis transmembrane conductance regulator (CFTR). *J. Biol. Chem.* 288, 31177–31191.
- van de Weijer, M.L., Krshnan, L., Liberatori, S., Guerrero, E.N., Robson-Tull, J., Hahn, L., Lebbink, R.J., Wiertz, E., Fischer, R., Ebner, D., and Carvalho, P. (2020). Quality control of ER membrane proteins by the RNF185/membralin ubiquitin ligase complex. *Mol. Cell* 79, 768–781.e67.
- Patten, J.J., Keiser, P.T., Morselli-Gysi, D., Menichetti, G., Mori, H., Donahue, C.J., Gan, X., Valle, I.D., Geoghegan-Barek, K., Anantpadma, M., et al. (2022). Identification of potent inhibitors of SARS-CoV-2 infection by combined pharmacological evaluation and cellular network prioritization. *iScience* 25, 104925.
- Nieto-Torres, J.L., Dediego, M.L., Alvarez, E., Jiménez-Guardeño, J.M., Regla-Nava, J.A., Llorente, M., Kremer, L., Shuo, S., and Enjuanes, L. (2011). Subcellular location and topology of severe acute respiratory syndrome coronavirus envelope protein. *Virology* 415, 69–82.
- Martinez-Ortiz, W., and Zhou, M.M. (2020). Could PROTACs protect us from COVID-19? *Drug Discov. Today* 25, 1894–1896.
- Simonetta, K.R., Taygerly, J., Boyle, K., Basham, S.E., Padovani, C., Lou, Y., Cummins, T.J., Yung, S.L., von Soly, S.K., Kayser, F., et al. (2019). Prospective discovery of small molecule enhancers of an E3 ligase-substrate interaction. *Nat. Commun.* 10, 1402.

STAR★METHODS

KEY RESOURCES TABLE

REAGENT or RESOURCE	SOURCE	IDENTIFIER
Antibodies		
Rabbit polyclonal GFP	Cell Signaling Technology	Cat#2555S
Rabbit RNF185 Polyclonal Antibody	ThermoFisher Scientific	Cat#PA5-78615
Mouse beta-actin Antibody	Cell Signaling	#3700
Bacterial and virus strains		
Stbl3	ThermoFisher Scientific	Cat#C737303
SARS-CoV-2 WA (hCoV-19/USA-WA1/2020)	BEI	Cat#NR-52281
SARS-CoV-2 Beta (B.1.351, hCoV-19/South Africa/KRISP-K005325/2020)	BEI	Cat#NR-55282
SARS-CoV-2 Delta (B.1.617, hCoV-19/USA/MA-NEIDL-01399/2021)	Dr. John H. Connor	N/A
Chemicals, peptides, and recombinant proteins		
MG132	Selleckchem	Cat#S2619
TAK (MLN7243)	Selleckchem	Cat#S8341
Pevonedistat (MLN4924)	Selleckchem	Cat#S7109
TRizol LS	Ambion	10296028
Chloroform/Isoamyl Alcohol	Acros Organics	327155000
Isopropanol	Fisher Bioreagents	BP2618-1
Ethanol	Fisher Bioreagents	BP2818-500
Critical commercial assays		
Cell Navigator® Live Cell Endoplasmic Reticulum (ER) Staining Kit *Blue Fluorescence*	AAT Bioquest	Cat#22636
Luna Universal Probe One Step RT-qPCR Kit	NEB	Cat#E3006
2019-nCoV RUO Kit	IDT	Cat#10006713
TransIT-L-LT1 Transfection Reagent	Mirus	Cat # MIR 2300
Experimental models: Cell lines		
Human: HEK293T-cas9	Broad Institute	https://www.atcc.org/products/crl-3216
Human: K562-cas9	Broad Institute	https://www.atcc.org/products/ccl-243
Human: A549-cas9	Broad Institute	https://www.atcc.org/products/ccl-185
Human: A549	ATCC	Cat#CCL-185
African Green Monkey Kidney: VeroE6	ATCC	Cat#CRL-1586
Oligonucleotides		
sgRNA sequence: RNF185_A Forward: CACCGCATCTTACCTGATGTAACA Reverse: AAACTGTTTACATCAGGTAAGATGC	IDT	N/A
sgRNA sequence: RNF185_B Forward: CACCGCTGAGAACTCCAGTGACGGG Reverse: AAACCCCTGCACTGGAGTTCTCAGC	IDT	N/A

(Continued on next page)

Continued

REAGENT or RESOURCE	SOURCE	IDENTIFIER
sgRNA sequence: RNF185_C Forward: CACCGGAGACCAGACCTAACAGAC Reverse: AAACGTCTGTTAGGTCTGGTCTCCC	IDT	N/A
sgRNA sequence: RNF185_D Forward: CACCGGTGCCACACAGGCTGATGA Reverse: AAACTCATCAGCCTGTGTGGCCACC	IDT	N/A
sgRNA sequence: SYVN1_A Forward: CACCGCCTCCAGAGTGAGAACCCT Reverse: AAACAGGGTTCTCACTCTGAGGC	IDT	N/A
sgRNA sequence: SYVN1_B Forward: CACCGTTGACTCACAAAGTCCACA Reverse: AAACTGTGGACTTTGTGAGTCAAGC	IDT	N/A
sgRNA sequence: SYVN1_C Forward: CACCGGTATGGAAAATGTGGTTGCA Reverse: AAACTGCAACCACATTTTCCATACC	IDT	N/A
sgRNA sequence: TMEM259_A Forward: CACCGACACGCAGGATGCCCTCACG Reverse: AAACCGTGAGGGCATCCTGCGTGTG	IDT	N/A
sgRNA sequence: TMEM259_B Forward: CACCGCAAGCCGCCGAGTAGCACAG Reverse: AAACCTGTGCTACTCGGCGGCTTGC	IDT	N/A

Recombinant DNA

Cilantro 2	Addgene	Plasmid #74450
Bison sgRNA library	Addgene	Cat# 169942
lentiCas9-Blast	Addgene	Cat# 52962
lentiGuide-Puro	Addgene	Cat# 52963

Software and algorithms

FlowJo™10	BD Biosciences	N/A
ImageJ	N/A	https://imagej.nih.gov/ij/
R	https://www.r-project.org/	https://www.r-project.org/
R Studio	https://www.rstudio.com/products/rstudio/download/	https://www.rstudio.com/products/rstudio/download/

RESOURCE AVAILABILITY

Lead contact

Further information and requests for resources and reagents should be directed to and will be fulfilled by the lead contact, Mikołaj Słabicki (slabicki@broadinstitute.org).

Material availability

Plasmids and all unique reagents generated in this study are available from the [lead contact](#) with a completed material transfer agreement.

Data and code availability

- Additional Supplemental Items are available from Mendeley Data at <https://data.mendeley.com/datasets/h6rn55h86x/1>.
- All data reported in this paper will be shared by the [lead contact](#) upon request.
- This paper does not report original code.
- Any additional information required to reanalyze the data reported in this paper is available from the [lead contact](#) upon request.

EXPERIMENTAL MODEL AND SUBJECT DETAILS

Cell lines

HEK293T-Cas9 and Vero E6 cells were cultured in DMEM (Gibco) and A549-Cas9, K562-Cas9 cells were grown in RPMI (Gibco), both supplemented with 10% fetal bovine serum (FBS) (Invitrogen), glutamine (Invitrogen), and penicillin-streptomycin (Invitrogen) at 37°C and 5% CO₂.

Generation of stability constructs

SARS-CoV-2 proteins ([Table S1](#)) were synthesized and cloned by Twist Bioscience into 'Cilantro2' vector (Addgene 74450, PGK target-eGFP-IRES-mCherry, puromycin resistance).

Lentivirus production

In a 96-well plate format, 11,000 HEK293T cells were seeded per well in 100 μL medium. The next day, 0.1 μL of TransIT-LT1 (Mirus, MIR2305) was added to 5 μL of OPTI-MEM (Invitrogen), incubated for 5 min at room temperature and combined with a mixture containing 28.9 ng of the SARS-CoV-2 - eGFP fusion protein stability plasmid, 166.7 ng psPAX2 and 16.7 ng pVSV-G in 3.3 μL OPTI-MEM. The solution was incubated for 30 min at room temperature and 10 μL was added to HEK293T cells in a dropwise manner. The lentivirus containing medium was collected two days after transfection and stored at -80 °C.

Lentiviral transduction

Cells were transduced by spin infection. 30,000 cells per well in 100 μL of culture medium was transferred to a well of a 96-well plate. 20% (v/v) of virus was added, which typically results in infection of 10–20% of cells (MOI 0.1–0.23). The plates were centrifuged for 2 h (2,200 rpm, 37°C). Two days post infection, cells were selected with puromycin at a concentration of 2 μg/mL.

SARS-CoV-2 stability assay

A total of 1.2×10^5 HEK293T-Cas9 cells stably expressing a SARS-CoV-2 stability construct were seeded in 96-well plate. 24 h post seeding, cells were either untreated, treated with 1 μM E1 inhibitor (MLN7243), treated with 10 μM 26S proteasome inhibitor treated (MG132), or treated with 1 μM neddylation inhibitor (MLN4924). 6 h post treatment, cells were detached using Trypsin (Gibco) and analyzed by flow cytometry on the BD LSRFortessa. Mean eGFP/mCherry signal was calculated using FlowJo and subsequently normalized to the DMSO treated sample of each reporter. All degradation assays in HEK293T were performed in triplicate, in A549 in four replicates, and in K562 in six replicates. Geometric means of eGFP and mCherry fluorescent signals for live and mCherry-positive cells were exported using flow cytometry analysis software (FlowJo, BD Biosciences). Ratios of eGFP to mCherry were normalized to the average of DMSO-treated controls.

BISON SARS-CoV-2 reporter screen in HEK293T cells

The BISON CRISPR library targets 713 E1, E2, and E3 ubiquitin ligases, deubiquitinates, and control genes, contains 2,852 sgRNAs, and was cloned into the pXPR003 vector as previously described.²⁰ The virus for the library was produced in a T-175 flask format, as described above in 'lentivirus production' with the following adjustments: 1.8×10^7 HEK293T cells in 25 mL complete DMEM medium, 244 μ L TransIT-LT1, 5 mL OPTI-MEM, 32 μ g of library, 40 μ g psPAX2 and 4 μ g pVSV-G in 1 mL OPTI-MEM. Ten per cent (v/v) of BISON CRISPR library was added (MOI \sim 0.5–0.7) to a 6-well plate of 2.2×10^6 HEK293T-Cas9 cells in 2 mL of cell culture medium per well, repeated for each stability construct. Cells were spin infected (2200 rpm, 2 h at 37°C) and selected with 2 μ g/mL puromycin 24 h post transduction. On the eighth day, cells were sorted on a Sony MA900 Multi-Application Cell Sorter using fluorescence-activated cell sorting (FACS). Four populations were collected (top 5%, top 5–10%, bottom 5–10% and bottom 5%) based on the eGFP/mCherry ratio. For each condition, at least 100×10^6 cells were subjected to sorting. Sorted populations were collected by centrifugation (5000 rpm, 5 min) and their cell pellets were flash-frozen in dry ice. Sorted cell pellets were resuspended in 100 μ L direct lysis buffer (1 mM CaCl₂, 3 mM MgCl₂, 1 mM EDTA, 1% Triton X-100, Tris pH 7.5) with freshly supplemented 0.2 mg/mL proteinase K. Lysates were incubated at 65°C for 15 min then 95°C for 10 min. A 25 μ L volume of this mix was used for library amplifications in each sorted sample in a 50 μ L reaction volume 0.04U Titanium Taq (Takara Bio 639210), 0.5 \times Titanium Taq buffer, 800 μ M dNTP mix, 200 nM P5-SBS3 forward primer, 200 nM SBS12-pXPR003 reverse primer), 94°C for 5 min, 15 cycles of [94°C for 30 s, 58°C for 15 s, 72°C for 30 s], 72°C for 2 min. Two microlitres of the first PCR reaction was used as the template for 15 cycles of the second PCR, in which Illumina adapters and barcodes were added (0.04U Titanium Taq (Takara Bio 639210), 1 \times Titanium Taq buffer, 800 μ M dNTP mix, 200 nM SBS3-Stagger-pXPR003 forward primer, 200 nM P7-barcode-SBS12 reverse primer). An equal amount of all samples was pooled and subjected to preparative agarose electrophoresis followed by gel purification (Qiagen). Eluted DNA was further purified by NaOAc and isopropanol precipitation. Amplified sgRNAs were quantified using the Illumina NextSeq platform.

Data analysis of CRISPR-Cas9 knockout screens

Our data analysis pipeline consisted of the following steps: (1) Normalize each sample to the total number of reads. (2) For each guide, calculate the ratio of reads in the stable versus unstable sorted gate and rank the sgRNAs. (3) Sum the ranks for each guide across all replicates. (4) Determine the gene rank as the median rank of the four guides targeting it. (5) Calculate p values by simulating a distribution with guide RNAs that have randomly assigned ranks over 100 iterations. The R scripts for these steps were previously published.²⁰

Generation of CRISPR-Cas9 knock-out cells

sgRNAs targeting genes of interest were cloned into the sgRNA.EFS.tBFP vector using BsmBI digestion as previously described.²⁰ Stability reporter cell lines were transduced in a 96-well plate as described above. Successful guide integration was confirmed by expression of BFP protein by flow cytometry using the BD LSRFortessa.

Immunoblots

Whole cell protein lysates were mixed with Laemmli (SDS-sample) buffer (reducing, 6X) (Boston BioProducts) and resolved on a polyacrylamide gel along with GFP pulldown lysates described above. The gel was transferred to a membrane and immunoblotted for GFP and HA as previously described.²¹

Transient transfection

5 μ g of iRFP720 tagged RNF185 plasmid was combined with 500 μ L of OptiMEM. 15 μ L of Mirus TransIT1 is added to the plasmid OptiMEM mix and incubated at room temperature for 30 min. This transfection mix was added to 1.6×10^6 cells in a 6-well plate. Fluorescence signal is observed 48 h post transfection using fluorescence microscopy.

Fluorescence microscopy

HEK293T cells expressing SARS-CoV-2 Envelope – eGFP were plated into a 96-well plate at 10,000 cells/well and transiently transfected with RNF185-iRFP720 construct as described above. Two days following transfection, cells were stained with Cell Navigator Live Cell Endoplasmic Reticulum (ER) working solution

(blue fluorescence) for 30 min at 37°C. Cells were imaged on a confocal microscope with SARS-CoV-2 Envelope in the GFP channel, RNF185 in the far-red channel, and the ER in the DAPI channel.

Virus cultivation

Three strains of SARS-CoV-2 were used in this study: SARS-CoV-2 WA (2019-nCoV/USA-WA1/2020), B.1.351, designated variant Beta (hCoV-19/South Africa/KRISP-K005325/2020), and B.1.617, designated variant Delta (hCoV-19/USA/MA-NEIDL-01399/2021). WA and Beta were obtained from BEI, and Delta was obtained from Dr. John H. Connor at the NEIDL, Boston University. The viruses were grown by passaging twice on VeroE6 cells (African green monkey kidney cells, known to be naturally permissive to viral growth). VeroE6 cells were infected with an MOI of <0.01 and incubated for around 3 days, when cytopathology was noted. Samples of each stock were sequenced and showed no evidence of contaminants. Each stock was aliquoted into small tubes and stored at -80°C until needed. All live virus work was performed in the BSL4 laboratory at the NEIDL, Boston University.

Effect of RNF185 KO on SARS-CoV-2 replication

The evening before the experiment, 7.5×10^4 non-targeting (NT) and RNF185 KO in A549-ACE2 cell line were plated into wells of a 24 well plate in DMEM with 10% fetal bovine serum. Cells were challenged with SARS-CoV-2 WA, Beta, or Delta at an MOI of 0.1 in duplicate. The cells were placed at 37°C for 1 h, then the initial inoculum was removed, cells were washed with PBS, and fresh medium was added to the cells. After 3 days, 250 μ L of the supernatant was harvested and inactivated in 750 μ L of TRIzol LS to be removed from containment. Virus RNA was then extracted. In a fume hood, 200 μ L of chloroform/isoamyl alcohol was added to each sample. Tubes were mixed, incubated at room temperature for 5 min, and spun at 11,600 xg for 15 min at 4°C. The aqueous phases were transferred to fresh tubes containing 500 μ L isopropanol. Samples were incubated for 10 min, then centrifuged as before. The isopropanol was decanted, and RNA pellets were washed in 1 mL of cold 75% ethanol. Samples were centrifuged again at 10,000 xg for 5 min at 4°C. The ethanol was removed, RNA pellets were air dried, and then resuspended in 50 μ L nuclease-free water. For PCR analysis, the Luna Universal Probe One Step RT-qPCR Kit was used. Each reaction consisted of the following: 10 μ L 2X reaction mix (from kit), 1 μ L enzyme (from kit), 1 μ L primer/probe mix (see below), 1 μ L sample, and 7 μ L nuclease-free water (from kit). The PCR was performed with the following parameters: 55°C/10min >95°C/1 min > [95°C/10 s > 60°C/30 s]/40 cycles. The primer and probe sets were from 2019-nCoV RUO Kit and nCoV_N2 forward and reverse primers. The primer sequences were forward primer 2019-nCoV_N2-F 5'-GACCCCAAAATCAGCGAAAT-3', reverse primer 2019-nCoV_N2-R 5'-TCTGGTACTGCCAGTTGAATCTG-3', and probe 2019-nCoV_N2-P 5'-FAM-ACC CCG CAT TAC GTT TGG TGG ACC-BHQ1-3'. A standard curve was generated from a series of dilutions with known concentrations of genome copies and was used to equate Cq values to the concentration of genome equivalents in the supernatant. Each sample was run in duplicate and averaged for the analysis.